PNAS RESEARCH ARTICLE | MICROBIOLOGY

Heat shock potentiates aminoglycosides against gram-negative bacteria by enhancing antibiotic uptake, protein aggregation, and ROS

Boyan Lv[a,1], Xuebing Huang[a,1], Chenchen Lijia[a], Yuelong Ma[a], Mengmeng Bian[a], Zhongyan Li[a], Juan Duan[b], Fang Zhou[c], Bin Yang[d], Xingwang Qie[e], Yizhi Song[e], Thomas K. Wood[f], and Xinmiao Fu[a,g,2]

Edited by Staffan Normark, Karolinska Institutet, Stockholm, Sweden; received October 10, 2022; accepted January 25, 2023

The potentiation of antibiotics is a promising strategy for combatting antibiotic-resistant/tolerant bacteria. Herein, we report that a 5-min sublethal heat shock enhances the bactericidal actions of aminoglycoside antibiotics by six orders of magnitude against both exponential- and stationary-phase *Escherichia coli*. This combined treatment also effectively kills various *E. coli* persisters, *E. coli* clinical isolates, and numerous gram-negative but not gram-positive bacteria and enables aminoglycosides at 5% of minimum inhibitory concentrations to eradicate multidrug-resistant pathogens *Acinetobacter baumannii* and *Klebsiella pneumoniae*. Mechanistically, the potentiation is achieved comprehensively by heat shock-enhanced proton motive force that thus promotes the bacterial uptake of aminoglycosides, as well as by increasing irreversible protein aggregation and reactive oxygen species that further augment the downstream lethality of aminoglycosides. Consistently, protonophores, chemical chaperones, antioxidants, and anaerobic culturing abolish heat shock-enhanced aminoglycoside lethality. We also demonstrate as a proof of concept that infrared irradiation- or photothermal nanosphere-induced thermal treatments potentiate aminoglycoside killing of *Pseudomonas aeruginosa* in a mouse acute skin wound model. Our study advances the understanding of the mechanism of actions of aminoglycosides and demonstrates a high potential for thermal ablation in curing bacterial infections when combined with aminoglycosides.

bacterial persister | antibiotic adjuvant | antibiotic resistance | reactive oxygen species | photothermal therapeutic material

Significance

Bacterial antibiotic resistance has become a severe threat to human and animal health. Increasing the efficacy of existing antibiotics is a promising strategy against antibiotic resistance. Here, we report that thermal treatment dramatically enhances the efficacy of aminoglycoside antibiotics in killing various bacteria, including multidrug-resistant pathogens. Mechanistically, such potentiation effect of thermal treatment is achieved by promoting the bacterial uptake of and enhancing the downstream lethality of aminoglycosides. Our study demonstrates a high potential of thermal treatment in curing antibiotic-resistance–associated bacterial infections when combined with aminoglycosides, thus expanding on its current application in treating tumors.

The discovery and application of antibiotics are regarded as the greatest medical breakthrough of the 20th century (1, 2). Nevertheless, widely spreading bacterial antibiotic resistance has become a severe threat to public health worldwide and led to 4.95 million deaths associated with the resistance in 2019, including 1.27 million deaths attributable to antibiotic resistance (3). Antibiotic resistance is achieved through various molecular mechanisms, including alteration or bypass of the drug target, production of antibiotic -modifying enzymes, decreased drug uptake, and increased drug efflux (4, 5). Besides these, bacteria can also survive the attack of bactericidal antibiotics by existing in certain physiological states, such as biofilms and persisters, which are highly tolerant and/or persistent to antibiotics (6–8). As such, biofilms and persisters play important roles in the evolution of antibiotic resistance, the relapse of chronic infections, and the failure of antibiotic treatments (6, 8–10).

We are well within the era of antibiotic resistance. Comprehensive strategies are needed to contain this public health crisis, including preventing or slowing antibiotic resistance, effectively killing antibiotic-resistant/tolerant pathogens, and mitigating the side effects and economic cost of antibiotic chemotherapy. While the discovery and development of new drugs are always the first defense line (5), extending the lifetime and increasing the efficacy of existing antibiotics are vital. In the past decades, significant achievements have been made to potentiate existing antibiotics using chemical adjuvants, which are nonantibiotic molecules but can facilitate antibiotics to kill bacteria (4, 11). These adjuvants can specifically inactivate drug-modifying enzymes (12), boost/reprogram bacterial metabolism (13–19), or interact with host defense mechanisms (4, 20).

In contrast to chemical adjuvants that have been investigated extensively, physical approaches for antibiotic potentiation have yet to be explored, and only a few cases have been reported. Falghoush et al. found that osmotic compounds could potentiate typical antibiotics against *Acinetobacter baumannii* biofilms (21). We previously observed that hypoionic shock (i.e., treatment with ion-free solutions) and rapid freezing dramatically potentiate aminoglycosides against bacterial persisters by activating mechanosensitive

Author contributions: X.F. designed research; B.L., X.H., C.L., Y.M., M.B., Z.L., and J.D. performed research; X.Q., and Y.S. contributed new reagents/analytic tools; B.L., F.Z., T.K.W., and X.F. analyzed data; F.Z. managed the project; B.Y. provided clinically isolated strains and performed antibiotic sensitivity assay; T.K.W. revised the manuscript and provided insightful comments; and B.L. and X.F. wrote the paper.

The authors declare no competing interest.

This article is a PNAS Direct Submission.

[1]B.L. and X.H. contributed equally to this work.

[2]To whom correspondence may be addressed. Email: xmfu@fjnu.edu.cn.

This article contains supporting information online at https://www.pnas.org/lookup/suppl/doi:10.1073/pnas.2217254120/-/DCSupplemental.

Published March 14, 2023.

channels and enhancing antibiotic uptake (22–26). In addition, photothermal materials have been developed to potentiate various antibiotics by imposing chemical and physical effects (27). Herein, we show that sublethal heat shock markedly and also specifically potentiates aminoglycoside killing of various *Escherichia coli* persisters and a broad-spectrum of gram-negative pathogens in vitro, as well as *Pseudomonas aeruginosa* in vivo. This work dissects the underlying molecular mechanism for heat shock-induced aminoglycoside potentiation and demonstrates a high potential of the combined treatment for curing bacterial infections.

Results

Sublethal Heat Shock Enhances the Bactericidal Action of Aminoglycosides against Both Stationary- and Exponential-Phase *E. coli* Cells. We previously reported that rapid freezing (e.g., 10-s freezing with liquid nitrogen) and 1-min hypoionic shock remarkably potentiate aminoglycoside in killing *E. coli* cells (22, 23, 26). We thus sought to examine whether other physical stress conditions could do the same. To this end, we found that heat shock, but neither ultrasonication nor ultraviolet irradiation, could facilitate aminoglycoside antibiotics (represented by tobramycin) to kill *E. coli* cells (*SI Appendix*, Fig. S1*A*).

Specifically, we observed that tobramycin treatment combined with a 5-min heat shock at 55 °C and 50 °C completely and moderately eradicated stationary-phase *E. coli* cells, respectively (lines 6 and 5 in Fig. 1*A*), whereas tobramycin treatment [at room temperature (RT)] or heat shock alone exhibited little or marginal bactericidal effects (lines 3 and 2). Notably, the killing effect became undetectable if tobramycin treatment was conducted post the heat shock or vice versa (*SI Appendix*, Fig. S1*B*), indicating that simultaneous rather than sequential treatments are essential. The killing effect of the combined treatment was time dependent (Fig. 1*B*) and temperature dependent (Fig. 1*A* and *SI Appendix*, Fig. S1 *C* and *D*). In addition, other types of aminoglycosides (i.e., streptomycin, kanamycin, and gentamicin) could also be potentiated in a concentration-dependent manner by a 5-min heat shock at 55 °C against both stationary- and exponential-phase *E. coli* cells (Fig. 1 *C* and *D*). In contrast, neither β-lactams (ampicillin) nor fluoroquinolones (ofloxacin) could be potentiated by heat shock. In contrast, neither β-lactams (ampicillin) nor fluoroquinolones (ofloxacin) could be potentiated by heat shock (Fig. 1 *C* and *D*), indicating that heat shock-induced potentiation is aminoglycoside specific. In line with this, the killing efficiency of penicillin at 55 °C against *E. coli* cells was reported to be less than one order of magnitude (28).

Heat Shock Potentiates Aminoglycosides to Kill Various *E. coli* Persisters. Next, we examined whether the combined treatment of aminoglycosides and heat shock could kill bacterial persisters, which have been shown to facilitate the evolution of antibiotic resistance (9, 29) and result in failing antibiotic chemotherapy (6, 10). First, we prepared persisters by pretreating the *E. coli* exponential-phase cell culture with ofloxacin or ampicillin for 3 h (30, 31). Cell survival assay revealed that around 1/10,000 of exponential-phase *E. coli* cells were ofloxacin-tolerant (*SI Appendix*, Fig. S2*A*), and more than 99.99% of these persisters could be killed by a subsequent 5-min combined treatment, but not by single treatment alone (Fig. 2*A*). Similarly, ampicillin-tolerant spontaneous persisters (*SI Appendix*, Fig. S2*B*) were also eliminated by the combined treatment (Fig. 2*B*).

Second, we examined protein synthesis arrest-induced persisters prepared by pretreatment with bacteriostatic antibiotics (32). *E. coli* exponential-phase cells, initially highly sensitive to tobramycin under conventional treatment conditions (i.e., agitation in Luria-Bertani (LB) medium for 1 h), became relatively tobramycin-tolerant after 1-h pretreatment with chloramphenicol, erythromycin, tetracycline, or rifampin (indicated by the red frame in *SI Appendix*, Fig. S2*C*). These chemically triggered persisters could be effectively

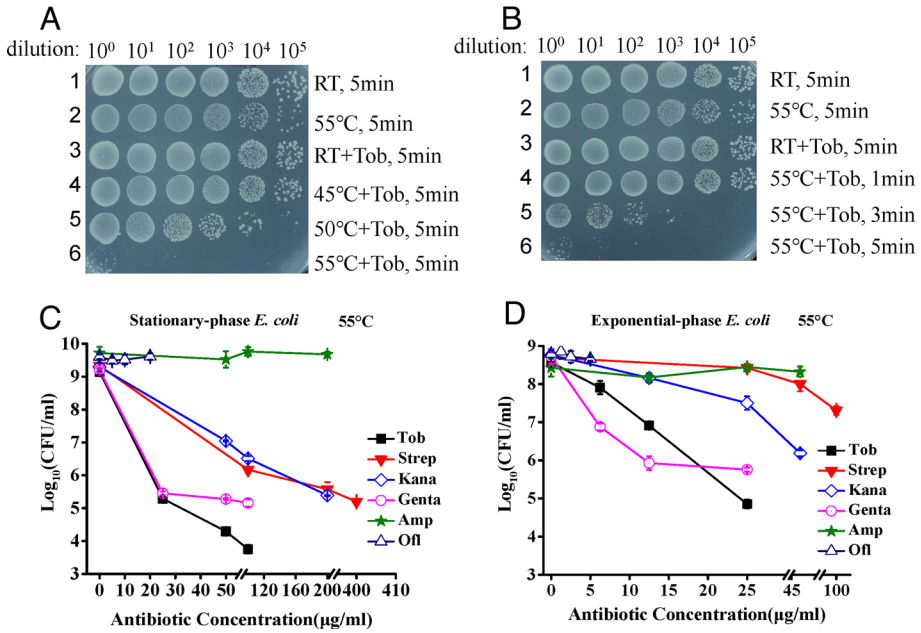

Fig. 1. Heat shock-induced aminoglycoside potentiation against *E. coli* cells. (*A*) Survival of *E. coli* stationary-phase cells following a 5-min combined treatment with 50 μg/mL Tob plus heat shock at 45 °C, 50 °C, or 55 °C (lines 4 to 6). (*B*) Survival of *E. coli* stationary-phase cells following combined treatment with 50 μg/mL Tob plus heat shock at 55 °C for varying times. (*C* and *D*) Survival of *E. coli* cells in stationary-phase (panel *C*) and exponential-phase (panel *D*) following a 5-min combined treatment with increasing concentrations of antibiotics plus heat shock at 55 °C. RT: room temperature. Data represent the mean ± SD of three replicates. Tob: tobramycin, Strep: streptomycin, Kana: kanamycin, Genta: gentamicin, Amp: ampicillin, Ofl: ofloxacin.

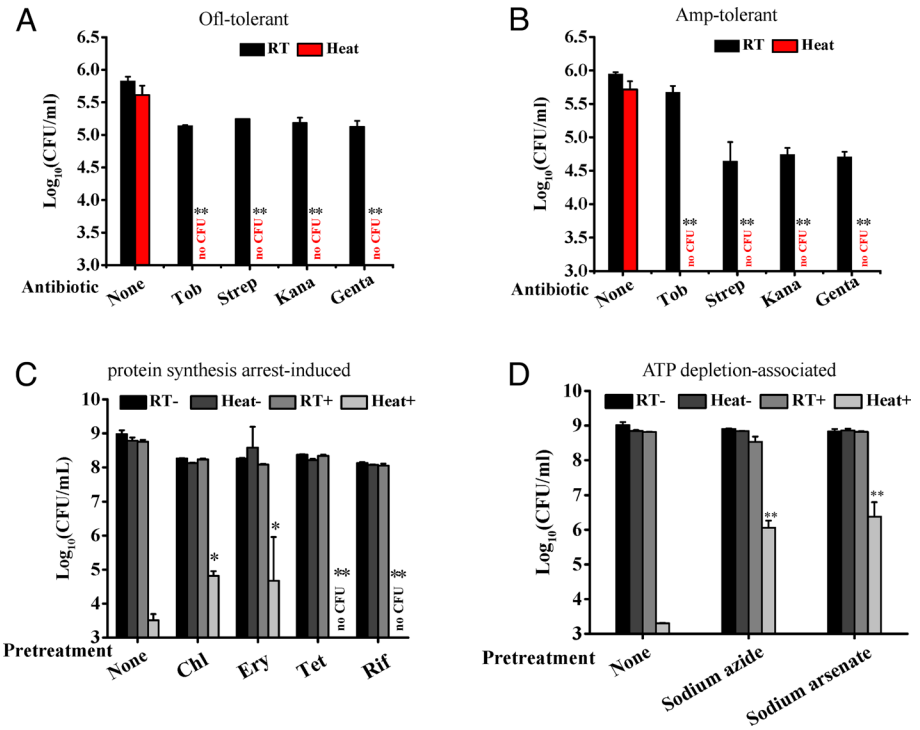

Fig. 2. Heat shock-induced aminoglycoside potentiation against various *E. coli* persisters. (*A* and *B*) Survival of Ofl-tolerant (panel *A*) and Amp-tolerant (panel *B*) *E. coli* spontaneous persisters following a 5-min combined treatment with indicated aminoglycoside plus heat shock at 55 °C (panel *A*) or 50 °C (panel *B*). Tob: 50 μg/mL; Strep: 200 μg/mL; Genta: 50 μg/mL; Kana: 100 μg/mL. (*C* and *D*) Survival of *E. coli* protein synthesis arrest-induced persisters (panel *C*) or ATP depletion-associated persisters (panel *D*) following a 5-min combined treatment with 25 μg/mL tobramycin plus heat shock at 55 °C. Persisters were prepared (refer to the *Materials and Methods*), and cell survival assay results are presented in *SI Appendix*, Fig. S2. Data represent the mean ± SD of three replicates. RT: room temperature; no CFU: no detectable CFU on the LB dish after 4 μL cell suspension was plated. ** and * indicates a *P*-value of <0.01 and <0.05 between antibiotic treatment at room temperature and the combined treatment, respectively.

killed by a 5-min combined treatment of heat shock and tobramycin (Fig. 2*C* and *SI Appendix*, Fig. S2*C*).

We further examined Adenosine Triphosphate (ATP) depletion-associated persisters (33), prepared by treating exponential-phase *E. coli* cells with sodium azide or arsenate. Treatment with these two chemicals made *E. coli* cells highly tolerant to tobramycin under conventional treatment conditions (the red frame in *SI Appendix*, Fig. S2*D*). Such tobramycin-tolerant *E. coli* persisters were effectively killed by the combined treatment with tobramycin and heat shock by around three orders of magnitude but hardly by a single treatment (Fig. 2*D* and *SI Appendix*, Fig. S2*D*). Nevertheless, the killing efficacy of the combined treatment against ATP depletion-associated *E. coli* persister cells was still much lower than that against normal cells (Fig. 2*D* and the blue frame in *SI Appendix*, Fig. S2*D*). Consistently, ATP levels in sodium azide- or sodium arsenate-treated *E. coli* cells were significantly decreased (*SI Appendix*, Fig. S2*E*). These observations suggest that heat shock-induced aminoglycoside potentiation partially depends on ATP.

Heat Shock Facilitates Aminoglycosides to Kill *E. coli* Clinical Isolates and Numerous Gram-Negative Bacteria, Including Multidrug-Resistant Pathogens. To explore the clinical potential of the combined treatment, we first examined clinically isolated strains of *E. coli* that were resistant to multitypes of antibiotics (*SI Appendix*, Table S3). Initially, we examined the sensitivity of these clinical strains to heat shock treatment at 55 °C or 50 °C and found that they were differentially sensitive to 55 °C (*SI Appendix*, Fig. S3*A*) but insensitive to 50 °C (*SI Appendix*, Fig. S3*B*). According to these results, we subjected all these strains to the combined treatment at 50 °C (*SI Appendix*, Fig. S3*C*), with six strains also being examined at 55 °C (*SI Appendix*, Fig. S3*D*). Cell survival assay revealed that 16 out of the 20 strains were sensitive to the combined treatment at 50 °C, and 3 out of the 6 strains were sensitive to the combined treatment at 55 °C (as summarized in *SI Appendix*, Table S3), illustrating the potential of the combined treatment in killing clinical multidrug resistant pathogens.

Second, we expanded our examination to other gram-negative pathogens (e.g., *P. aeruginosa*) as well as typical gram-positive pathogens (e.g., *Staphylococcus aureus*), whose sensitivity to each of the four types of aminoglycosides under conventional treatment conditions had been analyzed in our earlier report (23). We initially examined the sensitivity of these bacteria to heat shock treatment alone at 55 or 50 °C for varying times (*SI Appendix*, Fig. S4*A*), and an optimal temperature was chosen for the combined treatment (refer to *SI Appendix*, Table S4). Cell survival assay revealed that these pathogens in the stationary phase were differentially sensitive to the combined treatment (*SI Appendix*, Fig. S4 *B* and *C*), with the results being summarized in Table 1. In particular, whereas *P. aeruginosa* was highly sensitive to the combined treatment of heat shock with tobramycin, streptomycin, or gentamicin, *S. aureus* was hardly killed (Fig. 3*A*). It is important to note that *S. aureus* cells could be effectively killed by the combined treatment of these aminoglycosides with 5-methylindole or *n*-butanol as we recently reported (34, 35). Overall, gram-negative bacteria *Salmonella typhimurium, Aeromonas hydrophila*, *Shigella flexneri, Klebsiella pneumonia,* and *A. baumannii* were sensitive to the combined treatment of heat shock with one or multiple types of aminoglycosides, in contrast to gram-positive bacteria *Streptococcus pyogenes, Enterococcus faecalis* and *Micrococcus luteus* that were insensitive to the combined treatment of heat shock with any of the aminoglycosides (Table 1).

Notably, two multidrug-resistant pathogens, *K. pneumonia* KP-D367 and *A. baumannii* Ab6 could be effectively killed by

Table 1. Sensitivity of numerous bacteria to the combined treatment

Bacteria	Sensitivity*			
	Tob	Kana	Genta	Strep
E. coli	+++	+++	+++	+++
P. aeruginosa	+++	−	+++	++
A. baumannii	++	+	+	+
K. pneumoniae	++	−	+	+
A. hydrophila	++	+	++	++
S. typhimurium	+	+	+++	−
S. flexneri	++	++	+	−
S. aureus	−	−	−	−
S. pyogenes	−	−	−	−
M. luteus	−	−	−	−
E. faecalis	−	−	−	−

*Sensitivity of each bacterium to the combined treatment was determined by the cell survival assay as presented in Figs. 1*C* and 3*A*, and *SI Appendix*, Fig. S4 *B* and *C*. +++: highly sensitive; ++: moderately sensitive; +: slightly sensitive; -: insensitive.

the combined treatment using tobramycin of different concentrations plus heat shock at 50 °C (*SI Appendix*, Fig. S4*B*). By contrast, our recently developed aminoglycoside potentiation approaches using rapid freezing or hypoionic shock failed to facilitate tobramycin to kill these multidrug-resistant pathogens (23, 26). Given these, we further determined minimal inhibitory concentrations (MICs) of these pathogens to tobramycin, which were up to around 16,000 μg/mL (Fig. 3*B*). However, heat shock at 50 °C or 55 °C could potentiate tobramycin at concentrations below 800 μg/mL, or around 5% of their MICs, to effectively kill these two pathogens (Fig. 3*C*). In particular, the 3-min combined treatment with 400 μg/mL tobramycin at 55 °C could kill the pathogens by about two orders of magnitude (open circles and squares in Fig. 3*C*). In line with this result, we also observed that two tobramycin-resistant *E. coli* isolates were sensitive to the combined treatment with tobramycin plus heat shock (*SI Appendix*, Table S3).

Infrared Irradiation- or Photothermal Nanosphere-Induced Heat Shock Potentiates Aminoglycosides to Kill *P. aeruginosa* Cells in Mice. We next aimed to validate our approach in the animal model to prove the concept. *P. aeruginosa*, one of the most dangerous pathogens on the global priority list of antibiotic-resistant bacteria (36), was seeded in the skin wounds of mice for 1 h prior to treatment, as recently reported (37). To strictly control the temperature for heating wounds, we set up a special instrument system composed of an infrared lamp, a thermal meter, and a lifting platform (as diagrammed in Fig. 4*A* and *SI Appendix*, Fig. S5*A*).

Initially, we found that anesthetized mice with acute skin wounds could not endure infrared irradiation-induced thermal treatment at 55 °C for more than 2 min, i.e., mice would move, presumably due to thermal hurt on their acute skin wounds. Experimentally, we performed a 2-min combined treatment with 50 μg/mL tobramycin and heat shock at 55 °C in both the isolated skin model and acute skin wound model, although the in vitro killing efficiency of the 2-min combined treatment was far less than that for the 5-min combined treatment (*SI Appendix*, Fig. S5*B*). Cell survival assay revealed that the 2-min combined treatment killed *P. aeruginosa* seeded in the isolated skins more effectively than tobramycin treatment alone ($P < 0.0001$ in Fig. 4*B*), as well as the cells seeded in the acute wound of mice ($P < 0.0001$ in Fig. 4*C*). For comparison, the standard care treatment with 3% H_2O_2, though being able to eradicate *P. aeruginosa* cells under in vitro conditions completely (*SI Appendix*, Fig. S5*C*), exhibited moderate and little effects in the isolated skin model and acute skin wound model, respectively (Fig. 4 *B* and *C*), which is far less efficient than the 2-min combined treatment ($P < 0.0001$ in Fig. 4*B* and $P < 0.0001$ in Fig. 4*C*). No efficacy for 3% H_2O_2 treatment in the mouse model is presumably due to H_2O_2 deactivation by antioxidants or enzymes therein.

In retrospect, photothermal therapeutic materials have been developed in combination with antibiotics (e.g., aminoglycosides) to synergistically treat bacterial infections (27) through their multiple effects, which include damaging bacterial cell membranes (38–42), facilitating antibiotic release from liposome (39, 43), enhancing biofilm dispersion (38, 44), specifically targeting bacterial cells (38, 42, 43), and generating reactive oxygen species (ROS) (38). Here, we applied the previously reported dopamine-melanin colloidal nanospheres as activated by a near-infrared (808 nm) laser (45) to a certain heat shock temperature for potentiating aminoglycosides in the acute skin wound model, as illustrated in *SI Appendix*, Fig. S6*A*. First, cell survival assay revealed that such photothermal treatment achieved at 55 °C could dramatically potentiate tobramycin to kill *E. coli cells* in 96-well plates (*SI Appendix*, Fig. S6*B*). Second, we found that such photothermal treatment achieved at 50 °C could greatly potentiate tobramycin against *P. aeruginosa* in vitro. Its potentiation effect was even better than conventional heat shock (*SI Appendix*, Fig. S6*C*). Third, we demonstrated the effectiveness of this approach for *P. aeruginosa*

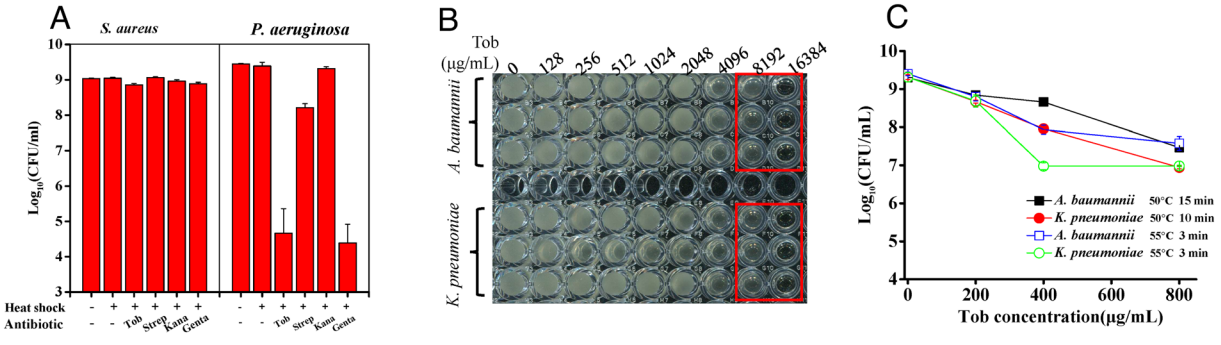

Fig. 3. Heat shock potentiates tobramycin against gram-negative pathogens. (*A*) Survival of *P. aeruginosa* and *S. aureus* cells following a 5-min combined treatment with indicated aminoglycosides plus heat shock at 55 °C (for *P. aeruginosa*) and 50 °C (for *S. aureus*). Tob: 50 μg/mL; Strep: 200 μg/mL; Genta: 50 μg/mL; Kana: 100 μg/mL. (*B*) MICs assay for *K. pneumonia* and *A. baumannii* toward tobramycin. (*C*) Survival of *K. pneumonia* and *A. baumannii* cells following the combined treatment with increasing concentrations of tobramycin plus indicated heat shock treatments. Data represent the mean ± SD of three replicates.

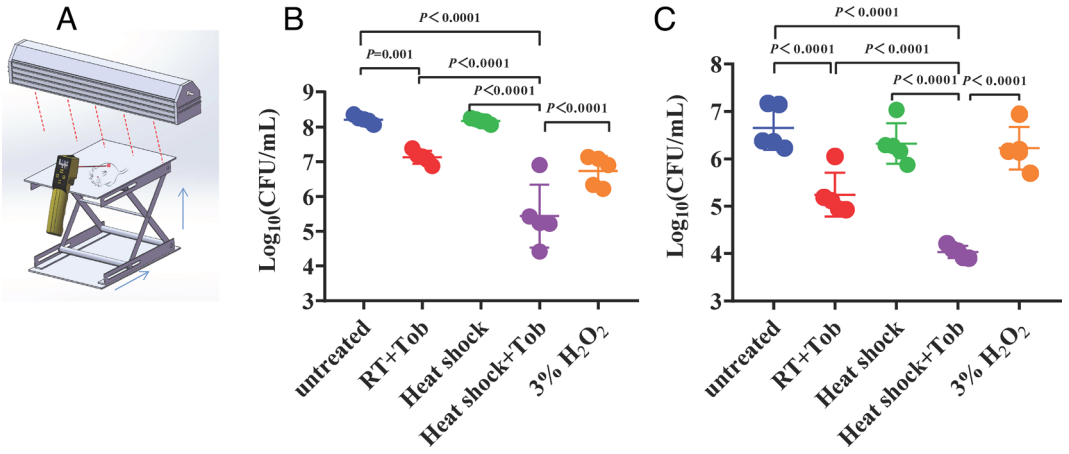

Fig. 4. Heat shock potentiates tobramycin killing of *P. aeruginosa* in mice. (*A*) Schematic diagram of the instrument system for animal experiments. (*B* and *C*) Survival of stationary-phase *P. aeruginosa* cells that were plated on a piece of mouse skin (panel *B*) or seeded in skin wounds of mice (panel *C*) for 1 h and then subjected to a 2-min combined treatment with 50 μg/mL tobramycin dissolved in 120 μL 0.9% NaCl solution plus infrared irradiation-controlled thermal treatment at 55 °C. The standard treatment with 3% H_2O_2 was studied for comparison, with its in vitro killing efficiency against *P. aeruginosa* presented in *SI Appendix*, Fig. S5*C*. Each circle represents the CFU value for one piece of skin or wound, and a short line indicates the average CFU for each group.

eradication in the isolated skin model (*SI Appendix*, Fig. S6*D*). Importantly, the 2-min combined treatment with tobramycin plus the photothermal nanosphere killed *P. aeruginosa* cells effectively in the acute skin wound model (*SI Appendix*, Fig. S6*E*), with the heat shock temperature (50 °C) being milder than that (55 °C) as achieved by the conventional infrared irradiation (Fig. 4*C*).

Heat Shock-Induced Aminoglycoside Potentiation Is Linked to the Enhanced Proton Motive Force (PMF) That Promotes the Bacterial Uptake of Aminoglycosides. To unveil the molecular mechanism underlying heat shock-induced aminoglycoside potentiation, we first examined *E. coli* strain MC4100, which carries a unique point mutation on the 30S ribosomal subunit protein S12 involved in aminoglycoside-binding and is highly resistant to streptomycin and moderately resistant to kanamycin (refer to *SI Appendix*, Fig. S7) but not to other aminoglycoside antibiotics (e.g., tobramycin). Cell survival assay revealed that MC4100 cells were effectively killed by the combined treatment of heat shock with tobramycin or gentamicin but not by that with streptomycin or marginally killed by that with kanamycin (Fig. 5*A*). In comparison, BW25113 cells were susceptible to the combined treatment of heat shock with each aminoglycoside (refer to Fig. 1*C*). These results indicate that heat shock-induced aminoglycoside potentiation relies on the actions of aminoglycosides on their conventional target ribosome.

The bacterial uptake of aminoglycosides is critical for aminoglycoside potentiation as elicited by metabolic recovery (13, 18, 46, 47), rapid freezing (26), hypoionic shock (23–25), or chemical induction (34, 35, 48). Therefore, we examined whether heat shock could enhance the bacterial uptake of aminoglycosides using tobramycin extraction coupled with cell-growth inhibition assay, a recently explored method (26). Cell-growth inhibition assay revealed that tobramycin, as extracted from heat-shocked *E. coli* stationary-phase cells, significantly inhibited the growth of *E. coli* cells preseeded on LB agar dishes (line 3, Fig. 5*B*). In contrast, tobramycin as extracted from *E. coli* cells treated at room temperature did not produce significant inhibition zones (line 2). These results are consistent with the cell survival assay (Fig. 1*A*) and indicate that heat shock could enhance the bacterial uptake of tobramycin.

Contrary to *E. coli* cells, we did not detect an appreciable cell growth inhibition zone by tobramycin as extracted from *S. aureus* cells regardless of heat shock (lines 7 and 8, Fig. 5*B*). In contrast, tobramycin as extracted from the *S. aureus* cells experiencing a combined treatment with tobramycin plus *n*-butanol significantly inhibited cell growth (line 9), consistent with our recently reported observation that *n*-butanol can potentiate tobramycin by enhancing antibiotic uptake (35). Therefore, the insensitivity of *S. aureus* to the combined treatment with tobramycin plus heat shock (Fig. 3*A*) is apparently due to the inability of heat shock to enhance the tobramycin uptake of *S. aureus*.

Considering that the bacterial uptake of aminoglycosides proceeds in a proton motive force (PMF)-dependent manner (13, 49), we examined whether the heat shock-enhanced tobramycin uptake resulted from an increase in PMF, which was measured by flow cytometric analysis using fluorescence probe 3,3′-Diethyloxacarbocyanine Iodide [DiOC2(3)]. Data presented in Fig. 5*C* indicate that heat shock significantly increased the PMF of stationary-phase *E. coli* cells, and this increase in PMF was diminished by pretreatment with CCCP, a widely used protonophore for dissipating PMF. Similarly, heat shock also enhanced the PMF of exponential-phase *E. coli* cells, and CCCP also diminished such an increase in PMF (*SI Appendix*, Fig. S8). In further support, we observed that heat shock-enhanced tobramycin lethality was nearly abolished by pretreatment with CCCP or its functional analog FCCP (Fig. 5*D*).

Irreversible Protein Aggregation Is Critical for Heat Shock-Enhanced Aminoglycoside Lethality. Besides the bacterial uptake of aminoglycosides, we further probed how heat shock affects the downstream lethality of aminoglycosides. We first examined metabolites among the cells experiencing different treatments (Fig. 6*A*). Metabolomic analyses revealed a few metabolites, including xanthosine, N6-methyladenosine, uridine, and guanosine, were up-regulated in the combined treatment cells. Among the down-regulated metabolites, betaine attracted our attention because it was reported as a chemical chaperone in suppressing protein aggregation (50), and protein aggregation has been reported to play a crucial role in aminoglycoside-induced lethality (51–53). We thus further examined the effect of betaine and other chemical chaperones (e.g., trimethylamine N-oxide (TMAO)) (54) on heat shock-enhanced aminoglycoside lethality. Cell survival assay revealed that these chemical chaperones, except for glycerine, could fully abolish the heat shock-enhanced

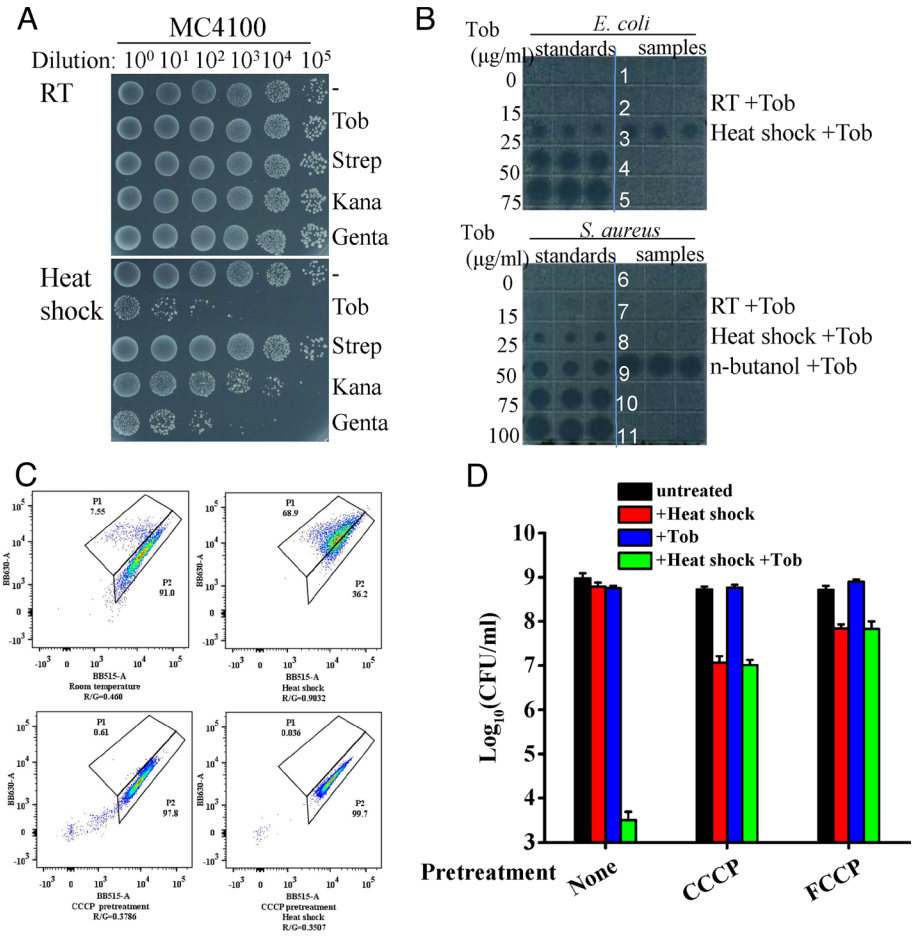

Fig. 5. Heat shock-induced tobramycin potentiation is linked to the enhanced tobramycin uptake. (*A*) Survival of *E. coli* MC4100 cells in the stationary phase following a 5-min combined treatment with indicated aminoglycoside plus heat shock at 55 °C. Tob: 50 μg/mL; Strep: 200 μg/mL; Genta: 50 μg/mL; Kana: 100 μg/mL. (*B*) *E. coli* inhibited by tobramycin was extracted from *E. coli* stationary-phase cells pretreated with 200 μg/mL tobramycin 55 °C for 5 min (*Upper* part) or from *S. aureus* cells pretreated with 200 μg/mL tobramycin at 50 °C for 5 min (*Lower* part). (*C*) Results of a flow cytometric analysis on the PMF of *E. coli* stationary-phase cells, which were pretreated or not with 20 μM Carbonyl Cyanide m-Chlorophenylhydrazone (CCCP) for 0.5 h and then heat shocked at 55 °C for 5 min before incubating with 30 μM DiOC2 (3) for analysis. The ratio of red to green fluorescence indicates the level of PMF and is designated at the bottom of each graph. (*D*) Survival of *E. coli* exponential-phase cells was agitated with 20 μM CCCP or Carbonyl cyanide 4-(trifluoromethoxy)phenylhydrazone (FCCP) for 0.5 h, followed by the 5-min combined treatments with 25 μg/mL tobramycin and heat shock.

tobramycin lethality against stationary-phase *E. coli* cells in a concentration-dependent manner (Fig. 6*B*).

The above observations implicate a role of protein aggregation in heat shock-enhanced aminoglycoside lethality. Therefore, we further isolated and characterized the protein aggregates in *E. coli* cells after different treatments. SDS-PAGE analysis results revealed much more protein bands present in the aggregates from the heat shock treated and the combined treatment cells than those from the untreated or tobramycin-treated cells (lanes 3 and 6 vs. lanes 1 and 2 in Fig. 6*C*). Notably, the accumulated protein aggregates in the combined treatment cells, if not decreased, became more abundant upon a 2-h recovery in LB medium (lanes 7 and 8 vs. lane 6). In contrast, heat shock-induced proteins' aggregates were substantially reduced to a basal level after the 2-h recovery (lane 5 vs. lane 1), which were most likely degraded and/or disaggregated, as implicated in an earlier report (55). Consistent with this observation, fluorescein isothiocyanate (FITC)-based microscopy analysis revealed that much more protein aggregates were formed in the combined treatment cells in comparison with those untreated cells or single treatment cells (Fig. 6*D*). Notably, the chemical chaperone TMAO-mediated protection on cell viability was accompanied with a significant reduction in the protein aggregates of *E. coli* cells, as revealed by FITC-based fluorescence microscopy analysis (Fig. 6*D*) and SDS-PAGE analysis (*SI Appendix*, Fig. S9*A*).

These observations suggest that irreversible protein aggregation causes heat shock-induced aminoglycoside lethality, as further supported by our following observations. First, the presence of metabolite betaine could not suppress the formation of protein aggregates during the combined treatment but rendered these preformed protein aggregates undetectable after a 2-h recovery (lane 11 vs. lane 10 in Fig. 6*C*). Meanwhile, the presence of betaine could fully protect *E. coli* cells from being killed by the combined treatment after 2-h recovery (*SI Appendix*, Fig. S9*B*). Second, we examined the sensitivity of *E. coli* HSP (heat shock protein) gene-deletion mutants to the combined treatment, given that HSPs play crucial roles in preventing protein aggregation and facilitating protein disaggregation (56). Among various HSP mutants, Δ*ibpA* and Δ*ibpB* were more sensitive to the combined treatment (*SI Appendix*, Fig. S9*C*), presumably due to their important roles in solubilizing protein aggregates formed in *E. coli* cells (57). Third, pretreatment of both stationary- and exponential-phase *E. coli* cells at sublethal heat shock temperature (44 °C) for 15 min could significantly help the cells to cope with the subsequent combined treatment of heat shock and tobramycin (Fig. 6*E*). Conceivably, heat shock pretreatment can up-regulate the expression of various HSPs (58, 59), which, in turn, ameliorate the subsequent combined treatment-induced protein aggregation and thus protect the cells.

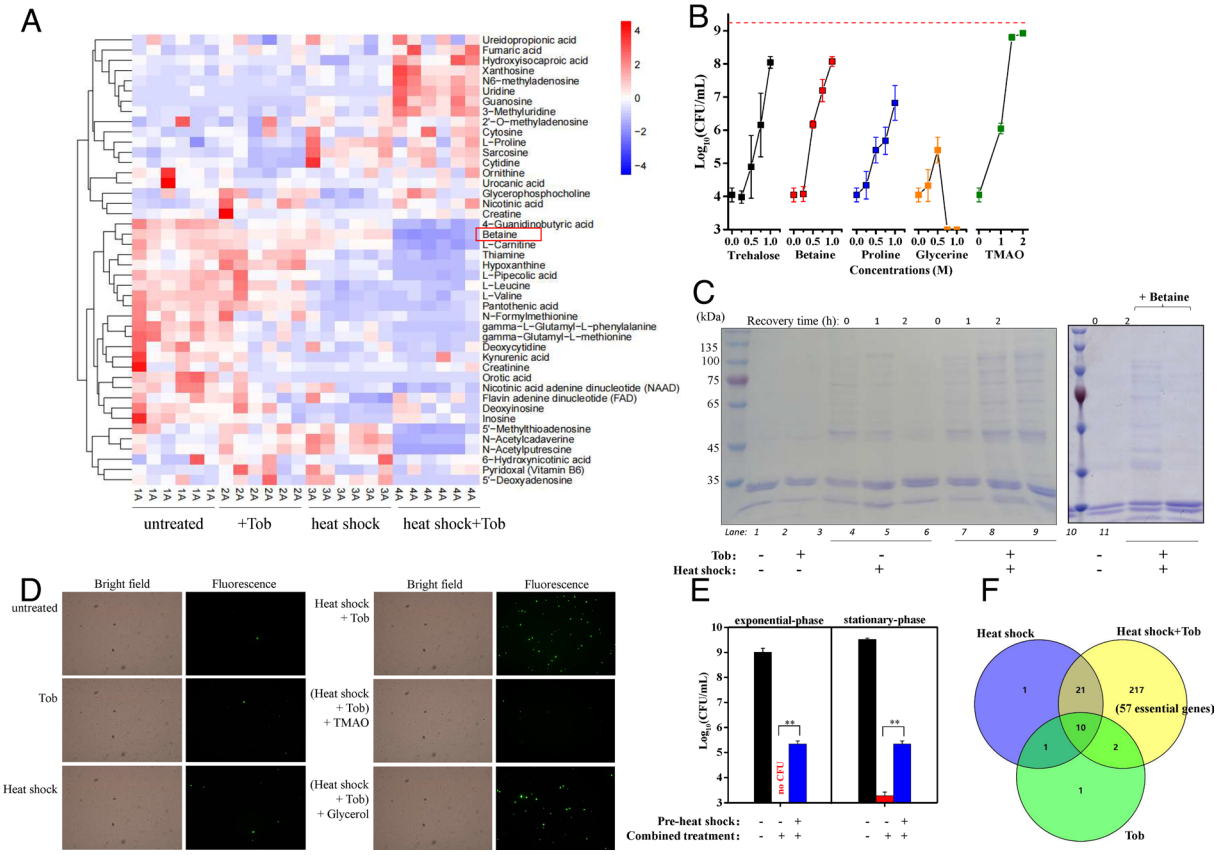

Fig. 6. Irreversible protein aggregation is critical for heat shock-induced tobramycin lethality. (*A*) Heatmap showing the relative abundance of various metabolites in *E. coli* cells after indicated treatments. Blue to red colors corresponds to low to high abundance, with betaine highlighted in red. (*B*) Survival of *E. coli* stationary-phase cells following the 5-min combined treatment in the absence or presence of indicated chemical chaperones. The dashed line presents the untreated cells. (*C*) SDS-PAGE analysis of protein aggregates isolated from stationary-phase *E. coli* cells. Cells were subjected to the 5-min combined treatment and then recovered in LB medium for 1 or 2 h. Lanes 10 to 11: The combined treatment was done in the presence of 1 M betaine with or without 2-h recovery. (*D*) Fluorescence microscopic imaging of stationary-phase *E. coli* cells following the 5-min combined treatment. Cells were incubated with 130 μM FITC for 15 min before imaging analysis. (*E*) Survival of *E. coli* stationary- and exponential-phase cells, which were heat shocked at 44 °C for 15 min followed by the 5-min combined treatment with 50 and 25 μg/mL tobramycin, respectively, plus heat shock at 55 °C. ** indicates $p<0.01$. (*F*) Protein profile of the protein aggregates isolated from *E. coli* cells experiencing tobramycin treatment alone, heat shock, and the combined treatment. A total of 217 proteins were specifically detected in the protein aggregates of cells experiencing the combined treatment, and 57 are products of essential genes (refer to Dataset S1).

To characterize the combined treatment-induced protein aggregates, we cut protein bands on the SDS-PAGE gel (*SI Appendix*, Fig. S9*D*) and then identified the proteins by liquid chromatography–mass spectrometry. A total of 250, 33, and 14 proteins were identified in the protein aggregates of the cells experiencing the combined treatment, heat shock treatment, and tobramycin treatment, respectively (Fig. 6*F*), with 217 proteins being specifically identified in the combined treatment cells (for detail, refer to Dataset S1). Among this specific proteome, there are 57 proteins assigned as the products of essential genes for *E. coli* (Dataset S1), and they are functionally involved in translation, gluconeogenesis, and DNA topological change. Loss of functions of these diversified essential proteins may contribute to heat shock-induced aminoglycoside lethality. Notably, several heat-shock chaperones (DnaK, ClpB, HtpG, and GroL), protease (Lon), and protease-associated proteins (ClpX, HslU) were detected in the aggregates (Dataset S1), consistent with the severe protein aggregation occurring in the cells.

A Critical Role of ROS for Heat Shock-Enhanced Aminoglycoside Lethality and Its Cross-Talk with Protein Aggregation. ROS have been shown to play crucial roles in the actions of bactericidal antibiotics, including aminoglycosides (60–63), although contradictory observations have also been reported (64, 65). Here, we present evidence to show that ROS is critical for heat shock-enhanced aminoglycoside lethality. First, we measured the level of ROS (represented by O_2^-) using the fluorescence probe dihydroethidium (DHE) (66). Both flow cytometry (Fig. 7*A*) and fluorescence microscopy analyses (*SI Appendix*, Fig. S10*A*) revealed a much higher level of O_2^- in the combined treatment *E. coli* cells than in the single treatment cells. Second, we examined the effect of a couple of antioxidants (e.g., vitamin C), ROS scavengers (e.g., lipoic acid and quercetin), and some compounds that promote the expression of endogenous antioxidant enzymes (e.g., N-acetyl-L-cysteine). Cell survival assay revealed that most of these compounds were able to abolish the heat significantly shock-induced tobramycin lethality (Fig. 7*B*). Third, taking tiron as an example of typical antioxidants, we demonstrated that it was able to dramatically decrease the level of O_2^- in the combined treatment cells (Fig. 7*A*). For comparison, 2,2′-dipyridyl, an iron chelator that was reported to suppress the bactericidal actions of aminoglycosides (60), neither protected the cells (Fig. 7*B*) nor reduced the level of O_2^- (Fig. 7*A*). Forth, we detected the presence of the antioxidant enzyme KatG in the protein aggregates of the combined treatment cells (Dataset S1) and observed an enhanced resistance of the cells overexpressing KatG or other antioxidant enzymes (AhpF and AhpC) against the combined treatment (*SI Appendix*, Fig. S10*B*). Notably, we did not observe a decrease in the catalase and superoxide dismutase activities of lysates from the combined treatment cells in comparison with the single treatment and untreated cells (*SI Appendix*, Fig. S10 *C* and *D*),

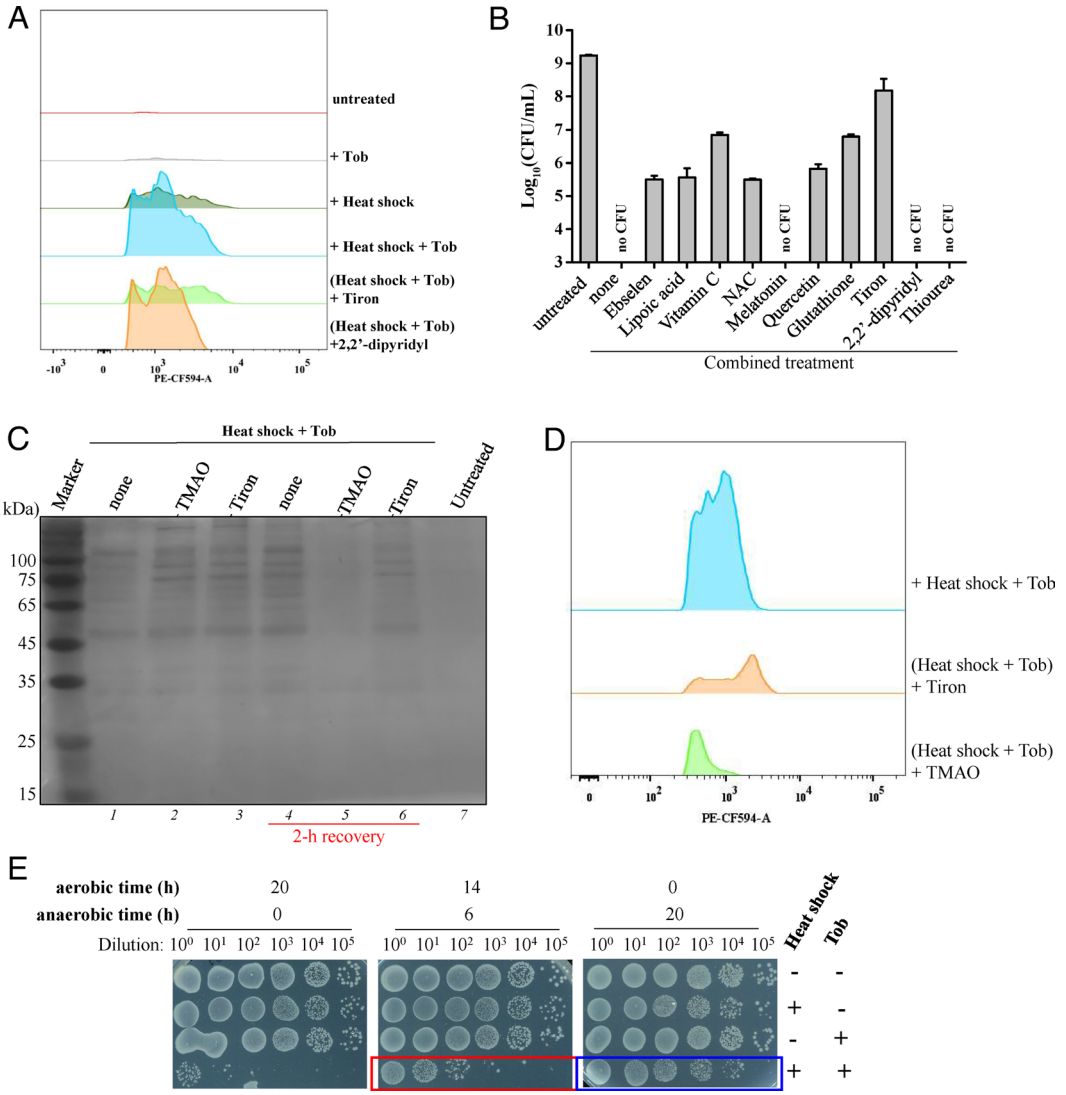

Fig. 7. ROS is critical for heat shock-induced tobramycin lethality and is largely induced by protein aggregation. (*A*) Flow cytometric analysis of *E. coli* stationary-phase cells following the 5-min combined treatment in the absence or presence of 0.04 mM 2,2′-bipyridyl or 2 mM tiron. Cells were incubated with 50 μM DHE for 90 min before analysis. (*B*) Survival of stationary-phase *E. coli* cells following the 5-min combined treatment (tobramycin plus heat shock at 55 °C) in the absence or presence of 100 μg/mL melatonin, 2 mM tiron, 10 mM L-glutathione, 40 mM vitamin C, 1 mM ebselen, 2 mM lipoic acid, 20 mM NAC, 0.5 mM quercetin, 225 mM thiourea or 0.04 mM 2,2′-bipyridyl. (*C*) SDS–PAGE analysis of protein aggregates isolated from stationary-phase *E. coli* cells, which were subjected to the 5-min combined treatment followed by recovery in LB medium for 2 h in the absence or presence of TMAO or tiron. (*D*) Flow cytometric analysis of stationary-phase *E. coli* cells following the 5-min combined treatment in the absence or presence of TMAO or tiron. Cells were incubated with DHE before analysis. (*E*) Survival of anaerobically cultured stationary-phase *E. coli* cells following the 5-min combined treatment (tobramycin plus heat shock at 55 °C). The anaerobic condition was achieved by either sequentially culturing the stationary-phase cells in an oxygen-free bag for 6 h or inoculating the cells in sealed Eppendorf tubes for 20 h.

suggesting that the increased ROS level in the combined treatment cells largely results from an increase in ROS generation rather than from a decrease in ROS degradation.

The essentiality of both protein aggregation and ROS to heat shock-enhanced aminoglycoside lethality prompted us to probe their relationship further. We examined the effect of the antioxidant tiron on protein aggregation and the effect of the chemical chaperone TMAO on ROS levels. SDS–PAGE analysis revealed that tiron only slightly attenuated the combined treatment-induced protein aggregation in cells after 2-h recovery (lane 6 vs. lane 4 in Fig. 7*C*), in contrast to TMAO that enabled the protein aggregates to become hardly detectable (lane 5 vs. lanes 4 and 2). On the other hand, flow cytometric analysis revealed that TMAO, similarly to tiron, was able to reduce the O_2^- effectively level in the combined treatment cells (Fig. 7*D*). Therefore, these observations suggest that ROS production is largely induced by protein aggregation and ROS also reciprocally but only slightly induces protein aggregation in the combined treatment cells, somehow in line with the general view that protein aggregation and ROS affect with each other (67).

Assuming that ROS is mainly produced by aerobic respiration (60, 68), we further compared the sensitivity of anaerobically and aerobically cultured *E. coli* cells. Cell survival assay revealed that two types of anaerobically cultured *E. coli* cells were more tolerant than the aerobically cultured ones to the combined treatment (Fig. 7*E*), particularly the *E. coli* cells cultured in sealed Eppendorf tubes (the blue frame in Fig. 7*E*). Together, these data further demonstrate that ROS is the primary lethal factor responsible for heat shock-induced aminoglycoside lethality.

Discussion

Sublethal Heat Shock Potentiates Aminoglycosides by Enhancing Antibiotic Uptake, Irreversible Protein Aggregation, and ROS Comprehensively. We propose a working model (Fig. 8) to illustrate the molecular mechanism underlying

heat shock-induced aminoglycoside potentiation based on the following observations. First, the killing effect of the combined treatment relies on the actions of aminoglycosides on their conventional target ribosome (Fig. 5*A*). Second, heat shock increases the PMF of bacterial cells (Fig. 5*C*), which, in turn, enhances the bacterial uptake of aminoglycosides (Fig. 5*B*), given that aminoglycoside uptake is well known to proceed in a PMF-dependent manner (13, 47, 49). Nevertheless, how heat shock enhances the PMF of *E. coli* cells remains unclear and merits further exploration. We propose that heat shock would globally shut down protein synthesis in *E. coli* cells (69) and thus greatly reduce ATP consumption, allowing the ATP synthase to hydrolyze yet-to-utilize cellular ATP to generate PMF. Third, heat shock combined with aminoglycoside dramatically enhances irreversible protein aggregation (Fig. 6*C*) and increases ROS levels (Fig. 7*A*), both of which are well known to generally contribute to aminoglycoside lethality (51–53, 60). Since heat shock alone could augment protein aggregation and ROS levels in *E. coli* cells, both of which are thus conceivably able to enhance aminoglycoside-induced protein aggregation and ROS synergistically. Notably, we observed a cross-talk between irreversible protein aggregation and ROS production, i.e., the former primarily drives the latter in the cells experiencing the combined treatment while the latter reciprocally but slightly induces the former (Fig. 7 *C* and *D*). Therefore, irreversible protein aggregation and ROS are primary upstream and downstream lethal factors in heat shock-enhanced aminoglycoside lethality, respectively (as illustrated in Fig. 8).

Overall, sublethal heat shock, which itself does not kill bacteria but can induce the heat shock response in bacteria (58), potentiates aminoglycosides not only by enhancing aminoglycoside uptake but also by augmenting the downstream lethal effects of the antibiotics (i.e., irreversible protein aggregation and ROS level), somehow similar to fumarate-enhanced TCA cycle activity (46). Nevertheless, the time for our approach is as short as 3 min, in contrast to fumarate-induced aminoglycoside potentiation, which requires a couple of hours to boost the TCA cycle and respiration. In retrospect, mild heat shock was reported to resensitize methicillin-resistant *S. aureus* to aminoglycosides by thermal deactivating a specific aminoglycoside-modifying enzyme in the bacterium (70), with the mechanism being distinct from that reported here. Extreme heat shock at 70 °C facilitated tobramycin and ciprofloxacin eradicating *P. aeruginosa* biofilms (71). In addition, no synergy was observed between heat shock and vancomycin (40), and less than one order of magnitude in killing efficiency was observed for penicillin and heat shock against *S. aureus* and *E. coli* cells (28).

Clinical Relevance of Heat Shock-Induced Aminoglycoside Potentiation. Aminoglycosides have been widely used since the 1940s (2), but antibiotic resistance and toxicity substantially limited their clinical applications. Overcoming the resistance and minimizing the toxicity are significant for applying this important class of bactericidal antibiotics to combat antibiotic-resistant/tolerant pathogens, particularly the gram-negative bacteria that are dominantly present on the priority list of antibiotic-resistant and death-leading pathogens (3, 36). In these respects, our approach,

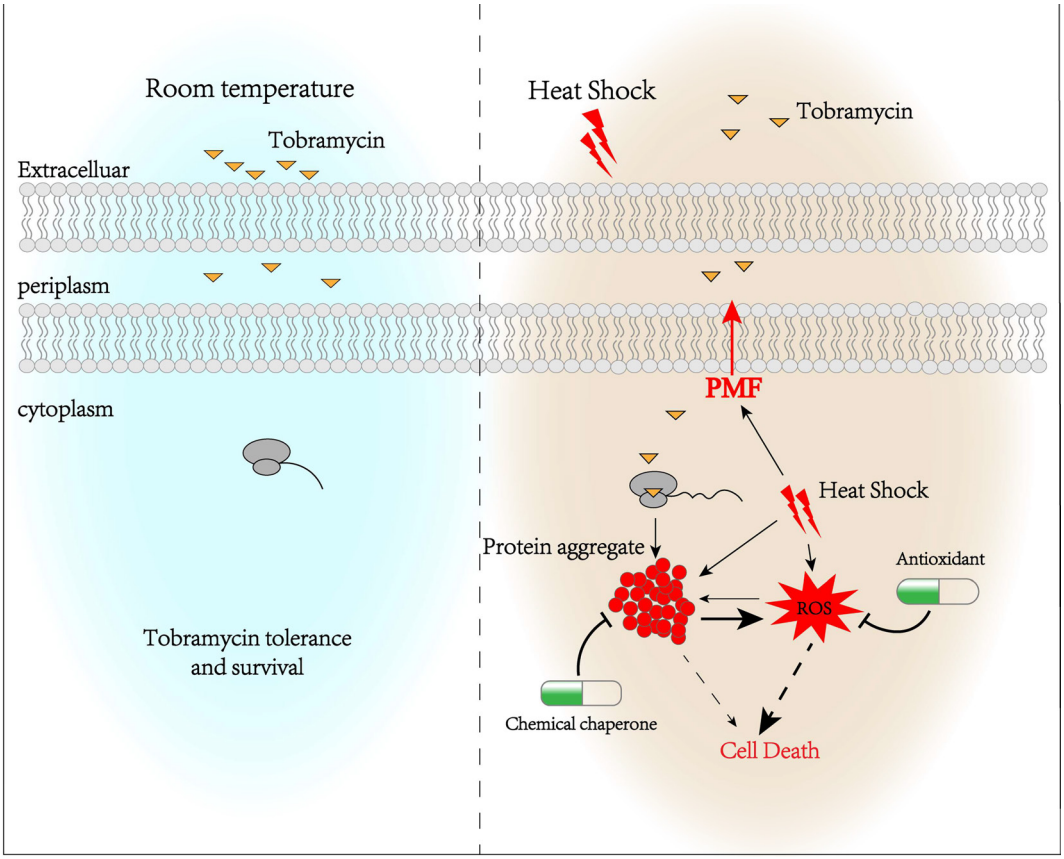

Fig. 8. Schematic illustration of the mechanism underlying heat shock-induced aminoglycoside potentiation against gram-negative bacteria. Heat shock imposes multiple effects on bacterial cells and aminoglycosides: 1) It increases the PMF of bacteria such that the bacterial uptake of aminoglycosides is enhanced; 2) it induces irreversible protein aggregation and abundant ROS (superoxide) when combined with aminoglycosides. Such dramatically augmented protein aggregation and ROS eventually lead to bacterial cell death. In addition, ROS, as produced by aerobic respiration, appears to be largely induced by protein aggregation, and the former reciprocally but slightly induces the latter and dominantly drives cell death.

though not effective against gram-positive bacteria, is of clinical significance based on the following considerations: 1) It can kill antibiotic-tolerant persister cells, which contribute to chronic and recurrent infections (6, 10); 2) it enables aminoglycosides at much lower concentrations than MICs to eradicate multidrug-resistant *A. baumannii* and *K. pneumoniae*, which are death-leading antibiotic-resistant pathogens (3); 3) the treatment lasts only a few minutes, which may also minimize the toxicity associated with aminoglycosides.

Our observation that 2-min infrared irradiation- or photothermal nanosphere-induced thermal treatment facilitated aminoglycosides to eradicate *P. aeruginosa* in a mouse acute skin wound model is therapeutically relevant. Nevertheless, this approach is not directly transferrable to clinics, mainly due to thermal injuries and the side effects of photothermal materials on human cells and tissues. Several directions merit further explorations for putting this approach forward to clinics. First, the temperature and duration of heat shock should be optimized for each bacterial pathogen regarding a specific aminoglycoside antibiotic, including tobramycin, gentamicin, kanamycin, streptomycin, netilmicin, amikacine, etimicin, isepamicin, and so on. As such, lower temperature and shorter duration of heat shock may be achieved concerning bacterium and aminoglycoside, and thermal injuries would be greatly reduced. Second, combining with photothermal nanomaterials that could be specifically delivered into bacterial infection sites (38, 42, 43) and efficiently absorb light from the near-infrared laser of ultra-low doses may ameliorate our approach and avoid damage to healthy tissues (27). Our observation illustrates the potential of this combination that dopamine-melanin colloidal nanosphere-induced thermal treatment, as achieved at 50 °C, has a comparable in vivo potentiation effect with the conventional infrared irradiation as achieved at 55 °C. Third, appropriate drugs for the remedy of thermal injuries, if used after the combined treatment, would also ameliorate the side effect of the approach. Lastly, the poor biocompatibility and cytotoxicity of photothermal materials and their degradation products are a potential issue, and organic small molecule-based photothermal materials appear to overcome these drawbacks because of their rapid excretion after treatment and excellent photothermal conversion efficiency (72, 73). We are currently exploring other photothermal nanomaterials, including carbon dots (74), to facilitate aminoglycosides to treat bacterial infections, particularly the infection by *P. aeruginosa* biofilms.

Materials and Methods

Strains, Culture Conditions, and Reagents. Bacterial strains used in this study that include *E. coli*, *P. aeruginosa*, *S. typhimurium*, *A. hydrophila*, *S. flexneri*, *K. pneumonia*, *A. baumannii*, *S. aureus*, *S. pyogenes*, *E. faecalis*, and *M. luteus* are listed in *SI Appendix*, Table S1. Briefly, an overnight culture of each strain was diluted at 1:500 in Luria-Bertani (LB) medium (the MRS medium was used for *E. faecalis*) and agitated in a shaker (37 °C, 220 rpm) for 20 to 24 h to prepare stationary-phase cells before antibiotic treatment. Antibiotics, chemical chaperones, and antioxidants used in this study are summarized in *SI Appendix*, Table S2. All chemical reagents are of analytical purity.

Combined Treatment with Aminoglycoside and Heat Shock. First, 100 μL *E. coli* cell cultures in exponential phase ($OD_{600} \approx 0.8$) were centrifuged (12,000 g, 1 min) in Eppendorf tubes, and the supernatant was completely removed. Then, cell pellets were thoroughly resuspended in 100 μL 0.9% NaCl solution containing aminoglycoside at concentrations as described in *SI Appendix*, Table S2 and further incubated at room temperature or heat shock temperatures (55 °C, 50 °C, 45 °C) for varying times. The cell suspension was washed twice with phosphate-buffered saline (PBS: 0.27 g/L KH_2PO_4, 1.42 g/L Na_2HPO_4, 8 g/L NaCl, 0.2 g/L KCl, pH 7.4) by centrifugation (12,000 g, 1 min), and then 4 μL 10-fold serially diluted cell suspension was spot plated onto LB agar dishes for survival assay. In addition, 30 μL *E. coli* cells and other types of bacterial strains in the stationary phase were centrifuged, and the cells were treated the same way (note: different bacterial strains have different resistance to heat shock, and thus the time for heat shock treatment is different). The effect of chemical chaperones and antioxidants was examined by adding them to the working solution during treatments.

Preparation and Eradication of *E. coli* Persister Cells. Spontaneous persister cells were prepared by adding ampicillin or ofloxacin at a final concentration of 400 μg/mL and 0.5 μg/mL into *E. coli* late exponential-phase cell culture ($OD_{600} = 1.0$) and continuing agitation for 3 h. Protein synthesis arrest-induced persisters were prepared by agitating *E. coli* exponential-phase cell culture with 35 μg/mL chloramphenicol, 20 μg/mL erythromycin, 15 μg/mL tetracycline, or 100 μg/mL rifampicin for 30 min according to an earlier report (32). ATP depletion-associated persisters were prepared by agitating *E. coli* exponential-phase cell culture with NaN_3 (w/v 0.2%) or 5 mM Na_3AsO_4 for 1 h. These pretreated cells were centrifuged, and the cell pellets were then subjected to a 5-min combined treatment with aminoglycoside at 55 or 50 °C.

Animal Experiments. According to an earlier report (75), we used a skin acute wound model to validate the in vivo efficacy of the combined treatment. ICR male mice (8 wk; ~ 28 g) were purchased from the Animal Center of Fujian Medical University and maintained in the Animal Center of Fujian Normal University. After 1 or 2 d, housed mice were randomly divided into five groups for surgery experiments (Group A: treatment with 0.9% NaCl solution at room temperature; Group B: treatment with tobramycin alone in 0.9% NaCl solution at room temperature; Group C: treatment with 0.9% NaCl solution at 55 °C; Group D: treatment with tobramycin in 0.9% NaCl solution at 55 °C; Group E: treatment with 3% H_2O_2 solution at room temperature). The mice were anesthetized by intraperitoneal injection of 4% chloral hydrate, and the back center was shaved and disinfected, and then a 1 × 1 cm^2 whole skin section was removed to make an acute skin wound. Afterward, 5 μL stationary-phase *P. aeruginosa* cells [approximately 1.52×10^7 Colony-forming units (CFU)] were seeded on the wound and fully absorbed. After adding 120 μL working solution onto the wound site, a 2-min heat shock treatment at 55 °C was achieved by infrared irradiation, with the temperature of the wound being monitored by a thermal meter and finely tuned by lifting the platform (as illustrated in Fig. 4*A* and *SI Appendix*, Fig. S5*A*). The residue working solution was removed by absorbing it with medical cotton, and then mice were bandaged firmly with medical gauze and housed overnight. The whole scab on the wound site was removed and homogenized, with the lysate being spot-plated on LB agar dishes for bacterial survival assay.

ROS Assay. Dihydroethidium was used to monitor the level of superoxide, as previously reported (66). Stationary-phase *E. coli* cells experiencing the combined treatment were washed with PBS and then incubated with DHE (50 μM) in PBS at 37 °C for 90 min before being subjected to flow cytometric analysis with a FACSymphony™A5 (BD Biosciences) and fluorescence imaging with a 100× oil-immersion objective (OLYMPUS DP70).

Statistics. Colony-forming units from LB agar dishes during cell survival assay were counted, and cell density was calculated according to the dilution fold and volume of cell droplet. Independent experiments were performed at least three times. Statistical analysis was performed in the MicroOrigin software using the ANOVA algorithm at a significance level of 0.05.

Ethics Statement. The animal use protocol was approved by the Animal Ethics and Welfare Committee of Fujian Normal University (approval No.: IACUC 20190006) and performed following the National Standards of the People's Republic of China (GB/T 35892-2018: Laboratory animals-Guideline for ethical review of animal welfare; GB/T 35823-2018: Laboratory animals-General requirements for the animal experiment).

Transparency Declarations. None to declare.

Data, Materials, and Software Availability. All study data are included in the article, *SI Appendix* and Dataset S1.

ACKNOWLEDGMENTS. We thank Prof. Luhua Lai and Xiaoyun Liu and Dr. Xiaoyun Liu (both from Peking University), and Dr. Qingeng Huang (from Fujian Normal University) for their kindness in providing bacterial strains as described in *SI Appendix*, Table S1. We also thank Dr. Yajuan Fu (Fujian Normal University) for help in flow cytometric analysis and graduate students (Miss Shuting Shi) for assistance in performing experiments, and Shijun Zhao, Jiamian Li, and Shiying Wang (from Peking University) for exploring the heat shock conditions. This work was supported by research grants from the National Natural Science Foundation of China (No. 31972918 to X.F.) and the Natural Science Foundation of Fujian Province (No. 2021J02029 to X.F.).

Author affiliations: [a]Provincial University Key Laboratory of Cellular Stress Response and Metabolic Regulation, Key Laboratory of Optoelectronic Science and Technology for Medicine of Ministry of Education, College of Life Sciences, Fujian Normal University, Fuzhou City 350117, China; [b]Department of Biochemistry and Molecular Biology, School of Basic Medical Sciences, Fujian Medical University, Fuzhou City 350122, China; [c]Department of Pharmacy, Southern University of Science and Technology Hospital, Shenzhen City 518055, China; [d]Department of Laboratory Medicine, The First Affiliated Hospital of Fujian Medical University, Fuzhou 350122, China; [e]CAS Key Laboratory of Bio-Medical Diagnostics, Suzhou Institute of Biomedical Engineering and Technology, Chinese Academy of Sciences, Suzhou 215163, China; [f]Department of Chemical Engineering, Pennsylvania State University, University Park, PA 16802-4400; and [g]Engineering Research Center of Industrial Microbiology of Ministry of Education, Fujian Normal University, Fuzhou City 350117, China

1. A. Fleming, *Penicillin* (Nobel Lecture, 1945), https://www.nobelprize.org/uploads/2018/06/fleming-lecture.pdf. Accessed 2 September 2019.
2. S. A. Waksman, *Streptomycin: Background, Isolation, Properties, and Utilization* (Nobel Lecture, 1952), https://www.nobelprize.org/uploads/2018/06/waksman-lecture.pdf. Accessed 2 September 2019.
3. Antimicrobial Resistance Collaborators, Global burden of bacterial antimicrobial resistance in 2019: A systematic analysis. *Lancet* (2022).
4. G. D. Wright, Antibiotic adjuvants: Rescuing antibiotics from resistance. *Trends Microbiol.* **24**, 862–871 (2016).
5. K. Lewis, The science of antibiotic discovery. *Cell* **181**, 29–45 (2020).
6. R. A. Fisher, B. Gollan, S. Helaine, Persistent bacterial infections and persister cells. *Nat. Rev. Microbiol.* **15**, 453–464 (2017).
7. N. Q. Balaban *et al.*, Definitions and guidelines for research on antibiotic persistence. *Nat. Rev. Microbiol.* **17**, 441–448 (2019).
8. J. W. Costerton, P. S. Stewart, E. P. Greenberg, Bacterial biofilms: A common cause of persistent infections. *Science* **284**, 1318–1322 (1999).
9. J. Liu *et al.*, Effect of tolerance on the evolution of antibiotic resistance under drug combinations. *Science* **367**, 200–204 (2020).
10. J. A. Bartell *et al.*, Bacterial persisters in long-term infection: Emergence and fitness in a complex host environment. *PLoS Pathog* **16**, e1009112 (2020).
11. Y. Liu *et al.*, Antibiotic adjuvants: An alternative approach to overcome multi-drug resistant Gram-negative bacteria. *Crit Rev. Microbiol.* **45**, 301–314 (2019).
12. H. C. Neu, K. P. Fu, Clavulanic acid, a novel inhibitor of beta-lactamases. *Antimicrob. Agents Chemother.* **14**, 650–655 (1978).
13. K. R. Allison, M. P. Brynildsen, J. J. Collins, Metabolite-enabled eradication of bacterial persisters by aminoglycosides. *Nature* **473**, 216–220 (2011).
14. N. Barraud *et al.*, Mannitol enhances antibiotic sensitivity of persister bacteria in Pseudomonas aeruginosa biofilms. *PLoS One* **8**, e84220 (2013).
15. C. N. Marques *et al.*, The fatty acid signaling molecule cis-2-decenoic acid increases metabolic activity and reverts persister cells to an antimicrobial-susceptible state. *Appl. Environ. Microbiol.* **80**, 6976–6991 (2014).
16. A. Crabbe *et al.*, Host metabolites stimulate the bacterial proton motive force to enhance the activity of aminoglycoside antibiotics. *PLoS Pathog* **15**, e1007697 (2019).
17. M. Wang *et al.*, N-Acetyl-D-Glucosamine acts as adjuvant that re-sensitizes starvation-induced antibiotic-tolerant population of E. Coli to beta-Lactam. *iScience* **23**, 101740 (2020).
18. X. L. Zhao *et al.*, Glutamine promotes antibiotic uptake to kill multidrug-resistant uropathogenic bacteria. *Sci. Transl. Med.* **13**, eabj0716 (2021).
19. Y. Liu *et al.*, Bacterial metabolism-inspired molecules to modulate antibiotic efficacy. *J. Antimicrob. Chemother.* **74**, 3409–3417 (2019).
20. Y. Liu *et al.*, Metformin restores tetracyclines susceptibility against multidrug resistant bacteria. *Adv. Sci. (Weinh)* **7**, 1902227 (2020).
21. A. Falghoush *et al.*, Osmotic compounds enhance antibiotic efficacy against Acinetobacter baumannii biofilm communities. *Appl. Environ. Microbiol.* **83**, e01297–e012117 (2017).
22. L. Jiafeng, X. Fu, Z. Chang, Hypoionic shock treatment enables aminoglycosides antibiotics to eradicate bacterial persisters. *Sci. Rep.* **5**, 14247 (2015).
23. B. Lv *et al.*, Mechanosensitive channels mediate hypoionic shock-induced aminoglycoside potentiation against bacterial persisters by enhancing antibiotic uptake. *Antimicrob. Agents Chemother.* **66**, e01125–e01221 (2022).
24. Z. Chen *et al.*, Hypoionic shock facilitates aminoglycoside killing of both nutrient shift- and starvation-induced bacterial persister cells by rapidly enhancing aminoglycoside uptake. *Front. Microbiol.* **10**, 2028 (2019).
25. Y. Gao *et al.*, Gentamicin combined with hypoionic shock rapidly eradicates aquaculture bacteria in vitro and in vivo. *Front. Microbiol.* **12**, 641846 (2021).
26. Y. Zhao *et al.*, Rapid freezing enables aminoglycosides to eradicate bacterial persisters via enhancing mechanosensitive channel MscL-mediated antibiotic uptake. *mBio.* **11**, e03239–e03249 (2020).
27. J. Huo *et al.*, Emerging photothermal-derived multimodal synergistic therapy in combating bacterial infections. *Chem. Soc. Rev.* **50**, 8762–8789 (2021).
28. C. Zhang *et al.*, Polyphenol-assisted exfoliation of transition metal dichalcogenides into nanosheets as photothermal nanocarriers for enhanced antibiofilm activity. *Acs Nano* **12**, 12347–12356 (2018).
29. I. Levin-Reisman *et al.*, Antibiotic tolerance facilitates the evolution of resistance. *Science* **355**, 826–830 (2017).
30. C. Wiuff *et al.*, Phenotypic tolerance: Antibiotic enrichment of noninherited resistance in bacterial populations. *Antimicrob. Agents Chemother.* **49**, 1483–1494 (2005).
31. I. Keren *et al.*, Persister cells and tolerance to antimicrobials. *FEMS Microbiol. Lett.* **230**, 13–18 (2004).
32. B. W. Kwan *et al.*, Arrested protein synthesis increases persister-like cell formation. *Antimicrob. Agents Chemother.* **57**, 1468–1473 (2013).
33. B. P. Conlon *et al.*, Persister formation in Staphylococcus aureus is associated with ATP depletion. *Nat. Microbiol.* **1**, 16051 (2016).
34. F. Sun *et al.*, 5-methylindole potentiates aminoglycoside against gram-positive bacteria including Staphylococcus aureus persisters under hypoionic conditions. *Front. Cell Infect Microbiol.* **10**, 84 (2020).
35. B. Lv *et al.*, n-butanol potentiates subinhibitory aminoglycosides against bacterial persisters and multidrug-resistant MRSA by rapidly enhancing antibiotic uptake. *ACS Infect Dis.* **8**, 373–386 (2022).
36. E. Tacconelli *et al.*, Discovery, research, and development of new antibiotics: The WHO priority list of antibiotic-resistant bacteria and tuberculosis. *Lancet Infect Dis.* **18**, 318–327 (2018).
37. J. M. Stokes *et al.*, A deep learning approach to antibiotic discovery. *Cell* **181**, 475–483 (2020).
38. Y. Liu *et al.*, Enzyme-responsive mesoporous ruthenium for combined chemo-photothermal therapy of drug-resistant bacteria. *ACS Appl. Mater Interfaces* **11**, 26590–26606 (2019).
39. L. Zhang *et al.*, Photon-responsive antibacterial nanoplatform for synergistic photothermal-/pharmaco-therapy of skin infection. *ACS Appl. Mater Interfaces* **11**, 300–310 (2019).
40. D. F. Hu *et al.*, Photothermal killing of methicillin-resistant staphylococcus aureus by bacteria-targeted polydopamine nanoparticles with nano localized hyperpyrexia. *Acs Biomater. Sci. Eng.* **5**, 5169–5179 (2019).
41. G. Qing *et al.*, Thermo-responsive triple-function nanotransporter for efficient chemo-photothermal therapy of multidrug-resistant bacterial infection. *Nat. Commun.* **10**, 4336 (2019).
42. G. Gao *et al.*, Near-infrared light-controllable on-demand antibiotics release using thermo-sensitive hydrogel-based drug reservoir for combating bacterial infection. *Biomaterials* **188**, 83–95 (2019).
43. Z. Guo *et al.*, Multifunctional glyco-nanosheets to eradicate drug-resistant bacteria on wounds. *Adv. Healthc Mater* **9**, e2000265 (2020).
44. Y. Zhao *et al.*, Near-infrared light-activated thermosensitive liposomes as efficient agents for photothermal and antibiotic synergistic therapy of bacterial biofilm. *ACS Appl. Mater. Interfaces* **10**, 14426–14437 (2018).
45. Y. Liu *et al.*, Dopamine-melanin colloidal nanospheres: An efficient near-infrared photothermal therapeutic agent for in vivo cancer therapy. *Adv. Mater.* **25**, 1353–1359 (2013).
46. S. Meylan *et al.*, Carbon sources tune antibiotic susceptibility in Pseudomonas aeruginosa via tricarboxylic acid cycle control. *Cell Chem. Biol.* **24**, 195–206 (2017).
47. B. Peng *et al.*, Exogenous alanine and/or glucose plus kanamycin kills antibiotic-resistant bacteria. *Cell Metab.* **21**, 249–261 (2015).
48. L. C. Radlinski *et al.*, Chemical induction of aminoglycoside uptake overcomes antibiotic tolerance and resistance in Staphylococcus aureus. *Cell Chem. Biol.* **26**, 1355–1364 (2019).
49. H. W. Taber *et al.*, Bacterial uptake of aminoglycoside antibiotics. *Microbiol. Rev.* **51**, 439–457 (1987).
50. A. Natalello *et al.*, The osmolyte betaine promotes protein misfolding and disruption of protein aggregates. *Proteins* **75**, 509–517 (2009).
51. B. D. Davis, L. L. Chen, P. C. Tai, Misread protein creates membrane channels: An essential step in the bactericidal action of aminoglycosides. *Proc. Natl. Acad. Sci. U.S.A.* **83**, 6164–6168 (1986).
52. A. B. Lindner *et al.*, Asymmetric segregation of protein aggregates is associated with cellular aging and rejuvenation. *Proc. Natl. Acad. Sci. U.S.A.* **105**, 3076–3081 (2008).
53. J. Ling *et al.*, Protein aggregation caused by aminoglycoside action is prevented by a hydrogen peroxide scavenger. *Mol. Cell* **48**, 713–722 (2012).
54. P. Leandro, C. M. Gomes, Protein misfolding in conformational disorders: Rescue of folding defects and chemical chaperoning. *Mini Rev. Med. Chem.* **8**, 901–911 (2008).
55. E. W. Wallace *et al.*, Reversible, specific, active aggregates of endogenous proteins assemble upon heat stress. *Cell* **162**, 1286–1298 (2015).
56. K. Liberek, A. Lewandowska, S. Zietkiewicz, Chaperones in control of protein disaggregation. *EMBO J.* **27**, 328–335 (2008).
57. M. Matuszewska *et al.*, The small heat shock protein IbpA of Escherichia coli cooperates with IbpB in stabilization of thermally aggregated proteins in a disaggregation competent state. *J. Biol. Chem.* **280**, 12292–12298 (2005).
58. S. Lindquist, The heat-shock response. *Annu. Rev. Biochem.* **55**, 1151–1191 (1986).
59. F. D. Schramm, K. Schroeder, K. Jonas, Protein aggregation in bacteria. *FEMS Microbiol. Rev.* **44**, 54–72 (2020).
60. M. A. Kohanski *et al.*, A common mechanism of cellular death induced by bactericidal antibiotics. *Cell* **130**, 797–810 (2007).
61. D. J. Dwyer, M. A. Kohanski, J. J. Collins, Role of reactive oxygen species in antibiotic action and resistance. *Curr. Opin. Microbiol.* **12**, 482–489 (2009).
62. X. Wang, X. Zhao, Contribution of oxidative damage to antimicrobial lethality. *Antimicrob. Agents Chemother* **53**, 1395–1402 (2009).
63. Y. Hong *et al.*, Post-stress bacterial cell death mediated by reactive oxygen species. *Proc. Natl. Acad. Sci. U.S.A.* **116**, 10064–10071 (2019).
64. I. Keren *et al.*, Killing by bactericidal antibiotics does not depend on reactive oxygen species. *Science* **339**, 1213–1216 (2013).
65. Y. Liu, J. A. Imlay, Cell death from antibiotics without the involvement of reactive oxygen species. *Science* **339**, 1210–1213 (2013).
66. B. Kalyanaraman *et al.*, Recent developments in detection of superoxide radical anion and hydrogen peroxide: Opportunities, challenges, and implications in redox signaling. *Arch Biochem. Biophys.* **617**, 38–47 (2017).

67. L. van Dam, T. B. Dansen, Cross-talk between redox signalling and protein aggregation. *Biochem. Soc. Trans.* **48**, 379–397 (2020).
68. M. P. Brynildsen *et al.*, Potentiating antibacterial activity by predictably enhancing endogenous microbial ROS production. *Nat. Biotechnol.* **31**, 160–165 (2013).
69. Y. Zhan *et al.*, Ribosome profiling reveals genome-wide cellular translational regulation upon heat stress in Escherichia coli. *Genomics Proteomics Bioinformatics* **15**, 324–330 (2017).
70. L. Tan *et al.*, Overcoming multidrug-resistant MRSA using conventional aminoglycoside antibiotics. *Adv. Sci. (Weinh)* **7**, 1902070 (2020).
71. E. B. Ricker, E. Nuxoll, Synergistic effects of heat and antibiotics on Pseudomonas aeruginosa biofilms. *Biofouling* **33**, 855–866 (2017).
72. B. Guo *et al.*, Organic small molecule based photothermal agents with molecular rotors for malignant breast cancer therapy. *Adv. Funct. Mater.* **30**, 1907093 (2020).
73. Z. L. Ding *et al.*, Organic small molecule-based photothermal agents for cancer therapy: Design strategies from single-molecule optimization to synergistic enhancement. *Coord. Chem. Rev.* **464**, 21464 (2022).
74. X. Qie *et al.*, Design, synthesis, and application of carbon dots with synergistic antibacterial activity. *Front. Bioeng. Biotechnol.* **10**, 894100 (2022).
75. J. M. Davidson, Animal models for wound repair. *Arch Dermatol. Res.* **290**, S1–S11 (1998).